

Implementation of a Toffoli Gate with Superconducting Circuits

A. Fedorov,¹ L. Steffen,¹ M. Baur,¹ M.P. da Silva,^{2,3} and A. Wallraff¹

¹*Department of Physics, ETH Zurich, CH-8093 Zurich, Switzerland*

²*Disruptive Information Processing Technologies Group,*

Raytheon BBN Technologies, 10 Moulton Street, Cambridge, MA 02138, USA

³*Département de Physique, Université de Sherbrooke, Sherbrooke, Québec, J1K 2R1, Canada*

The Toffoli gate is a three-qubit operation that inverts the state of a target qubit conditioned on the state of two control qubits. It makes universal reversible classical computation [1] possible and, together with a Hadamard gate [2], forms a universal set of gates in quantum computation. It is also a key element in quantum error correction schemes [3–7]. The Toffoli gate has been implemented in nuclear magnetic resonance [3], linear optics [8] and ion trap systems [9]. Experiments with superconducting qubits have also shown significant progress recently: two-qubit algorithms [10] and two-qubit process tomography have been implemented [11], three-qubit entangled states have been prepared [12, 13], first steps towards quantum teleportation have been taken [14] and work on quantum computing architecture has been done [16]. Implementation of the Toffoli gate with only single- and two-qubit gates requires six controlled-NOT gates and ten single-qubit operations [15], and has not been realized in any system owing to current limits on coherence. Here we implement a Toffoli gate with three superconducting transmon qubits coupled to a microwave resonator. By exploiting the third energy level of the transmon qubits, we have significantly reduced the number of elementary gates needed for the implementation of the Toffoli gate, relative to that required in theoretical proposals using only two-level systems. Using full process tomography and Monte Carlo process certification, we completely characterized the Toffoli gate acting on three independent qubits, measuring a fidelity of 68.5 ± 0.5 per cent. A similar approach [16] realizing characteristic features of a Toffoli-class gate has been demonstrated with two qubits and a resonator and achieved a limited characterization considering only the phase fidelity. Our results reinforce the potential of macroscopic superconducting qubits for the implementation of complex quantum operations with the possibility of quantum error correction schemes [17].

We have implemented a Toffoli gate with three transmon qubits (A,B and C) dispersively coupled to a microwave transmission-line resonator, in a sample which is identical to the one used in ref. [14]. The resonator is

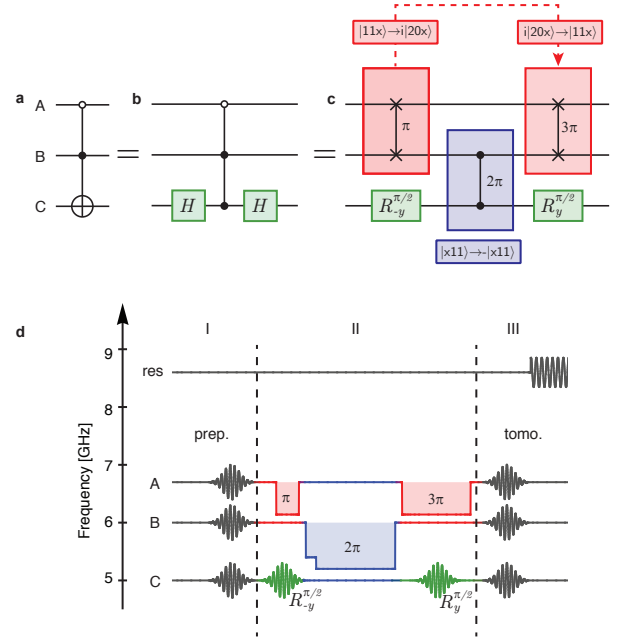


FIG. 1. **Circuit diagram of the Toffoli gate.** **a**, A NOT-operation (\oplus) is applied to qubit C if the control qubits (A and B) are in the ground (\circ) and excited state (\bullet) respectively. **b**, The Toffoli gate can be decomposed into a CPHASE gate sandwiched between Hadamard gates (**H**) applied to qubit C. **c**, The CPHASE gate is implemented as a sequence of a qubit-qutrit gate, a two-qubit gate and a second qubit-qutrit gate. Each of these gates is realized by tuning the $|11\rangle$ state into resonance with $|20\rangle$ for a $\{\pi, 2\pi, 3\pi\}$ coherent rotation respectively. For the Toffoli gate, the Hadamard gates are replaced with $\pm\pi/2$ rotations about the y axis (represented by $R_{\pm y}^{\pi/2}$). **d**, Pulse sequence used for the implementation of the Toffoli gate. During the preparation (I), resonant microwave pulses are applied to the qubits on the corresponding gate lines. The Toffoli gate (II) is implemented with three flux pulses and resonant microwave pulses (colour coded as in c). The measurement (III) consists of microwave pulses that turn the qubit states to the desired measurement axis, and a subsequent microwave pulse applied to the resonator is used to perform a joint dispersive read-out.

used for joint three-qubit read-out by measuring its transmission [18]. At the same time, it serves as a coupling bus for the qubits [19]. The qubits have a ladder-type energy level structure with sufficient anharmonicity to allow individual microwave addressing of different transitions. We use the first two energy levels as the computational

qubit states, $|0\rangle$ and $|1\rangle$, and use the second excited state, $|2\rangle$, to perform two-qubit and qubit-qutrit operations (a qutrit is a quantum ternary digit). From spectroscopy, we deduce a bare resonator frequency $\nu_r = 8.625$ GHz with a quality factor of 3300; maximum qubit transition frequencies $\nu_A^{\max} = 6.714$ GHz, $\nu_B^{\max} = 6.050$ GHz and $\nu_C^{\max} = 4.999$ GHz; and respective charging energies $E_c/h = 0.264, 0.296$ and 0.307 GHz (h , Planck's constant) and qubit-resonator coupling strengths $g/2\pi = 0.36, 0.30$ and 0.34 GHz for qubits A, B and C. At the maximum transition frequencies, we find respective qubit energy relaxation times of $T_1 = 0.55, 0.70$ and 1.10 μs and phase coherence times of $T_2^* = 0.45, 0.6$ and 0.65 μs for qubits A, B and C.

In the conventional realization of the Toffoli gate, a NOT operation is applied to the target qubit (C) if the control qubits (A, B) are in the state $|11\rangle$. In our set-up it is more natural to construct a variation of the Toffoli gate shown in Fig. 1a in which the state of the target qubit is inverted if the control qubits are in $|01\rangle$. This gate can easily be transformed to the conventional Toffoli gate by a redefinition of the computational basis states of qubit A or by applying two π -pulses on qubit A.

The Toffoli gate can be constructed from a 'controlled-controlled-phase' (CCPHASE) sandwiched between two Hadamard gates acting on the target qubit as shown in Fig. 1b. A CCPHASE gate leads to a phase shift of π for state $|1\rangle$ of the target qubit if and only if the control qubits are in state $|01\rangle$. In other words, this corresponds to a sign change of only one of the eight computational three-qubit basis states: $|011\rangle \leftrightarrow -|011\rangle$.

The basic idea of 'hiding' states by transforming them into non-computational states to simplify the implementation of a Toffoli gate was theoretically proposed in refs. 20 and 21 and has been experimentally implemented for linear optics and ion trap systems [8, 9]. The implementation of the scheme of ref. [20] in our set-up would require three controlled-phase (CPHASE) gates, six single-qubit operations and two single-qutrit operations. Instead, we construct the CCPHASE from a single two-qubit CPHASE gate and two qubit-qutrit gates. The latter gates are called π -SWAP and 3π -SWAP, respectively (Fig. 1c, red frames). The application of a

single CPHASE gate to qubits B and C (Fig. 1c, blue frame) inverts the sign of both $|111\rangle$ and $|011\rangle$. To create the CCPHASE operation, the computational basis state $|111\rangle$ is transferred to the non-computational state $i|201\rangle$ by the π -SWAP gate, effectively hiding it from the CPHASE operation acting on qubits B and C. After the CPHASE operation, $|111\rangle$ is recovered from the non-computational level $i|201\rangle$ by the 3π -SWAP gate. Alternative approaches using optimal control of individual qubits for implementing a Toffoli gate in a single step have been proposed [22] and recently analyzed in the context of the circuit quantum electrodynamics architecture [23].

All three-qubit basis states show three distinct evolution paths during our CCPHASE gate (Table 1). Only input state $|011\rangle$ is affected by the CPHASE gate acting on qubits B and C, which transfers $|011\rangle$ to the desired state, $-|011\rangle$. The states $|11x\rangle$ with $x \in \{0, 1\}$ are transferred by the π -CPHASE gate to the states $i|20x\rangle$. The subsequent CPHASE gate therefore has no influence on the state. The last gate (3π -CPHASE) transfers $i|20x\rangle$ back to $|11x\rangle$. Together the two SWAP gates realize a rotation by 4π , such that the state $|11x\rangle$ does not acquire any extra phase relative to the other states. The states of the last group ($|010\rangle$ and $|x0y\rangle$ with $y \in \{0, 1\}$) do not change during the CPHASE gate sequence.

The actual experimental implementation of the Toffoli gate consists of a sequence of microwave and flux pulses applied to the qubit local control lines (Fig. 1d). The arbitrary rotations about the x and y axis [24] are realized with resonant microwave pulses applied to the open transmission line at each qubit. We use 8-ns-long, Gaussian-shaped DRAG-pulses [24, 25] to prevent population of the third level and phase errors during the single-qubit operations. Few-nanosecond-long current pulses passing through the transmission lines next to the superconducting loops of the respective qubits control the qubit transition frequency realizing z -axis rotations. All two-qubit or qubit-qutrit gates are implemented by tuning a qutrit non-adiabatically to the avoided crossing between the states $|11x\rangle$ and $|20x\rangle$ or, respectively, $|x11\rangle$ and $|x20\rangle$ (refs 12, 26, and 27). During this time, the system oscillates between these pairs of states with respective frequencies $2J_{11,20}^{AB}$ and $2J_{11,20}^{BC}$. With interaction times $\pi/(2J_{11,20}^{AB}) = 7$ ns, $3\pi/(2J_{11,20}^{AB}) = 21$ ns and $\pi/(2J_{11,20}^{BC}) = 23$ ns, we realize a π -SWAP and a 3π -SWAP between qubits A and B and a CPHASE gate between qubits B and C, respectively. Our use of qubit-qutrit instead of single-qutrit operations allows for a more efficient construction of the Toffoli gate. Direct realization of the scheme proposed in ref. 20 in our system would require eight additional microwave pulses (used to implement six single-qubit and two single-qutrit gates) with a twofold increase in overall duration of the pulse sequence with respect to our scheme.

TABLE I. List of states after each step of the CCPHASE gate. The state $|011\rangle$ acquires a phase shift of π during the CPHASE pulse; the states $|11x\rangle$ are transferred to $i|20x\rangle$, 'hiding' them from the CPHASE gate; and the initial states $|x0y\rangle$ and $|010\rangle$ do not change during the sequence.

Initial state	After π -SWAP	After CPHASE	After 3π -SWAP
$ 011\rangle$	$ 011\rangle$	$- 011\rangle$	$- 011\rangle$
$ 11x\rangle$	$i 20x\rangle$	$i 20x\rangle$	$ 11x\rangle$
$ x0y\rangle$	$ x0y\rangle$	$ x0y\rangle$	$ x0y\rangle$
$ 010\rangle$	$ 010\rangle$	$ 010\rangle$	$ 010\rangle$

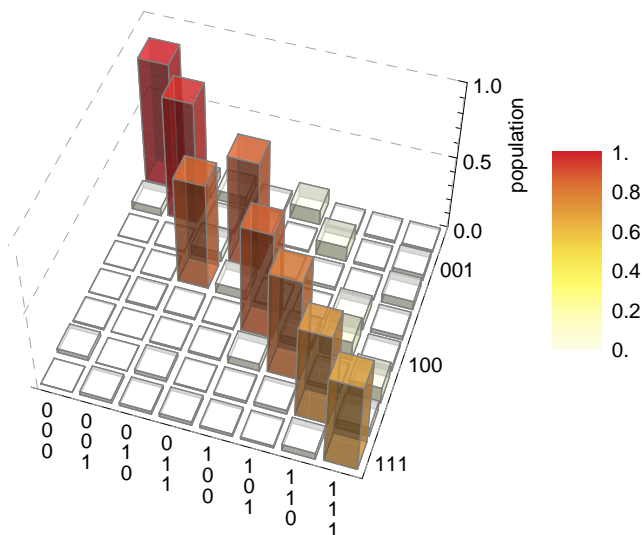


FIG. 2. **Truth table of the Toffoli gate.** The state of qubit C is inverted if qubits A and B are in the state $|01\rangle$. The fidelity of the truth table is $F = (1/8)\text{Tr}[U_{\text{exp}}U_{\text{ideal}}] = 76.0\%$

We have characterized the performance of this realization of a Toffoli gate by measuring the truth table, by full process tomography [28] and by Monte Carlo process certification [29, 30]. The truth table depicted (Fig. 2) shows the population of all computational basis states after applying the Toffoli gate to each of the computational basis states. It reveals the characteristic properties of the Toffoli gate, namely that a NOT operation is applied on the target qubit (C) if the control qubits (A and B) are in the state $|01\rangle$. The fidelities of the output states show a significant dependence on qubit lifetime. In particular, input states with qubit A (with the shortest lifetime) in the excited state generally have the worst fidelity, indicating that the protocol is mainly limited by the qubit lifetime. The fidelity of the measured truth table, U_{exp} , with respect to the ideal one, U_{ideal} , namely $F = (1/8)\text{Tr}[U_{\text{exp}}U_{\text{ideal}}] = 76.0\%$, shows the average performance of our gate when acting onto the eight basis states.

As an essential addition to the classical characterization of the gate by the truth table, we have performed full, three-qubit process tomography and reconstructed the process matrix, χ_{exp} , to characterize the quantum features of the Toffoli gate completely, overcoming the limited characterization provided by measurements of the phase fidelity only [16]. For this purpose, we prepared a complete set of 64 distinct input states by applying all combinations of single-qubit operations chosen from the set $\{\text{id}, \pi/2_x, \pi/2_y, \pi_x\}$ for each qubit, and performed state tomography on the respective output states. The process matrix reconstructed directly from the data has a fidelity of $F = \text{Tr}[\chi_{\text{exp}}\chi_{\text{ideal}}] = 70 \pm 3\%$ (the error represents a 90% confidence interval), where χ_{ideal} is the

ideal process matrix. Using a maximum-likelihood procedure [31] to correct for unphysical properties of χ_{exp} , we find that the obtained process matrix, $\chi_{\text{exp}}^{\text{ML}}$, has a fidelity of $F = \text{Tr}[\chi_{\text{exp}}^{\text{ML}}\chi_{\text{ideal}}] = 69\%$ with expected errors at the level of 3%. In Fig. 3a, χ_{exp} shows the same key features as χ_{ideal} (Fig. 3b).

To gain an accurate alternative estimate of the process fidelity without resorting to a maximum-likelihood procedure, we implemented Monte Carlo process certification following the steps described in ref. 29. First we define a Pauli observable as $\hat{P}_n = \prod_{j=1,\dots,6} \hat{p}_{n,j}$, a product of six single-qubit operators chosen from the set of the identity and the Pauli operators ($\hat{p}_{n,j} \in \{\mathbb{1}, \sigma_x, \sigma_y, \sigma_z\}$). Then we determine the 232 observables with non-vanishing expectation values $P_n = \text{Tr}[\hat{\rho}_T \hat{P}_n] \neq 0$, where $\hat{\rho}_T$ is the Choi matrix of the Toffoli process. For each \hat{P}_n we prepare all ($2^3 = 8$) eigenstates of the product of the first three operators comprising \hat{P}_n , apply the Toffoli operation to these states and measure the expectation value of the product of the last three operators in \hat{P}_n . Averaging over the results obtained with all eigenstates provides an estimate of P_n . Extracting all 232 expectation values in this way allows us to estimate the fidelity of the Toffoli gate as $68.5 \pm 0.5\%$ using Monte Carlo process certification, which is in good agreement with the fidelity evaluated using tomography.

The scheme that we use to implement the Toffoli gate is generic and can readily be applied to other systems because the majority of the quantum systems used as qubits have additional energy levels at their disposal. Reduction of the total gate time by use of qubit-qutrit gates together with the recent advances in the extension of the coherence times of the superconducting circuits [32, 33] indicates a path towards the realization of practical quantum error correction.

We thank Stefan Filipp, Alexandre Blais for useful discussions and Kiryl Pakrouski for his contributions in early stages of the experimental work. This work was supported by the Swiss National Science Foundation (SNF), the EU IP SOLID and ETH Zurich.

-
- [1] Toffoli, T. *Reversible computing*, vol. 85 of *Lecture Notes in Computer Science* (Springer Berlin / Heidelberg, 1980).
 - [2] Shi, Y. Both Toffoli and Controlled-NOT need little help to do universal quantum computation. *arXiv:0205115* (2002).
 - [3] Cory, D. G. *et al.* Experimental quantum error correction. *Phys. Rev. Lett.* **81**, 2152–2155 (1998).
 - [4] Knill, E., Laflamme, R., Martinez, R. & Negrevergne, C. Benchmarking quantum computers: The five-qubit error correcting code. *Phys. Rev. Lett.* **86**, 5811–5814 (2001).
 - [5] Chiaverini, J. *et al.* Realization of quantum error correction. *Nature* **432**, 602–605 (2004).
 - [6] Pittman, T. B., Jacobs, B. C. & Franson, J. D. Demon-

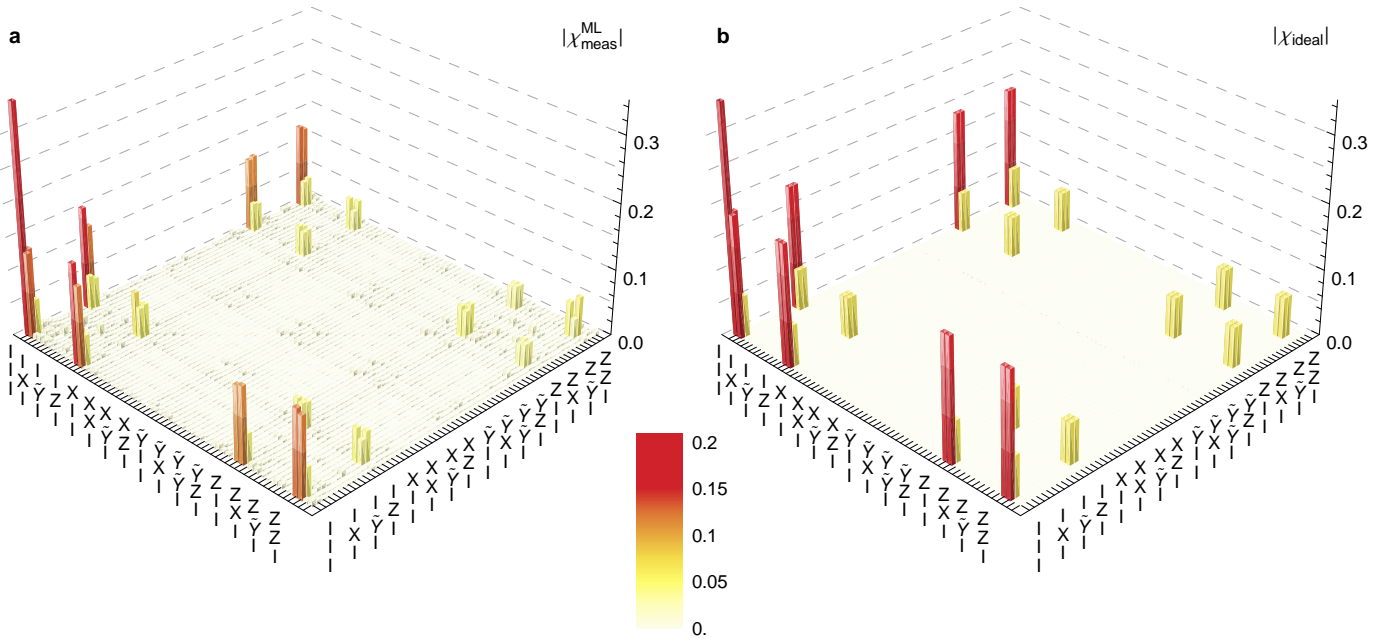


FIG. 3. **Process tomography of the Toffoli gate.** Bar chart of the absolute value of the measured process matrix $\chi_{\text{exp}}^{\text{ML}}$ (a) and the ideal process matrix χ_{ideal} (b). The elements are displayed in the operator basis $\{III, IIX, IIZ, \dots, ZZZ\}$, where I is the identity and $\{X, Y, Z\}$ are the Pauli operators $\{\sigma_x, -i\sigma_y, \sigma_z\}$. The fidelity of the process matrix is $F = \text{Tr}[\chi_{\text{exp}}^{\text{ML}} \chi_{\text{ideal}}] = 69\%$. The process fidelity estimated using the Monte Carlo certification method is $68.5 \pm 0.5\%$.

- stration of quantum error correction using linear optics. *Phys. Rev. A* **71**, 052332 (2005).
- [7] Aoki, T. *et al.* Quantum error correction beyond qubits. *Nat Phys* **5**, 541–546 (2009).
- [8] Lanyon, B. P. *et al.* Simplifying quantum logic using higher-dimensional hilbert spaces. *Nat. Phys.* **5**, 134–140 (2009).
- [9] Monz, T. *et al.* Realization of the quantum Toffoli gate with trapped ions. *Phys. Rev. Lett.* **102**, 040501 (2009).
- [10] DiCarlo, L. *et al.* Demonstration of two-qubit algorithms with a superconducting quantum processor. *Nature* **460**, 240–244 (2009).
- [11] Yamamoto, T. *et al.* Quantum process tomography of two-qubit controlled-z and controlled-not gates using superconducting phase qubits. *Phys. Rev. B* **82**, 184515 (2010).
- [12] DiCarlo, L. *et al.* Preparation and measurement of three-qubit entanglement in a superconducting circuit. *Nature* **467**, 574–578 (2010).
- [13] Neeley, M. *et al.* Generation of three-qubit entangled states using superconducting phase qubits. *Nature* **467**, 570–573 (2010).
- [14] Baur, M. *et al.* Benchmarking a teleportation protocol realized in superconducting circuits. Preprint at <http://arxiv.org/abs/1107.4774> (2011).
- [15] Barenco, A. *et al.* Elementary gates for quantum computation. *Phys. Rev. A* **52**, 3457–3467 (1995).
- [16] Mariani, M. *et al.* Implementing the quantum von neumann architecture with superconducting circuits. *Science* **334**, 61–65 (2011).
- [17] Reed, M. D. *et al.* Realization of Three-Qubit quantum error correction with superconducting circuits. Preprint at <http://arxiv.org/abs/1109.4948> (2011).
- [18] Filipp, S. *et al.* Two-qubit state tomography using a joint dispersive readout. *Phys. Rev. Lett.* **102**, 200402 (2009).
- [19] Majer, J. *et al.* Coupling superconducting qubits via a cavity bus. *Nature* **449**, 443–447 (2007).
- [20] Ralph, T. C., Resch, K. J. & Gilchrist, A. Efficient toffoli gates using qudits. *Phys. Rev. A* **75**, 022313 (2007).
- [21] Borrelli, M., Mazzola, L., Paternostro, M. & Maniscalco, S. Simple trapped-ion architecture for high-fidelity toffoli gates. *Phys. Rev. A* **84**, 012314 (2011).
- [22] Spörl, A. *et al.* Optimal control of coupled josephson qubits. *Phys. Rev. A* **75**, 012302 (2007).
- [23] Stojanovic, V. M., Fedorov, A., Bruder, C. & Wallraff, A. Quantum-control approach to realizing a toffoli gate in circuit QED. Preprint at <http://arxiv.org/abs/1108.3442> (2011).
- [24] Gambetta, J. M., Motzoi, F., Merkel, S. T. & Wilhelm, F. K. Analytic control methods for high-fidelity unitary operations in a weakly nonlinear oscillator. *Phys. Rev. A* **83**, 012308 (2011).
- [25] Motzoi, F., Gambetta, J. M., Reber, P. & Wilhelm, F. K. Simple pulses for elimination of leakage in weakly nonlinear qubits. *Phys. Rev. Lett.* **103**, 110501 (2009).
- [26] Strauch, F. W. *et al.* Quantum logic gates for coupled superconducting phase qubits. *Phys. Rev. Lett.* **91**, 167005 (2003).
- [27] Haack, G., Helmer, F., Mariani, M., Marquardt, F. & Solano, E. Resonant quantum gates in circuit quantum

- electrodynamics. *Phys. Rev. B* **82**, 024514 (2010).
- [28] Chuang, I. L. & Nielsen, M. A. Prescription for experimental determination of the dynamics of a quantum black box. *J. Mod. Opt.* **44**, 2455–2467 (1997).
- [29] da Silva, M. P., Landon-Cardinal, O. & Poulin, D. Practical characterization of quantum devices without tomography. *Phys. Rev. Lett.* (to appear). Preprint at <http://arxiv.org/abs/1104.3835> (2011).
- [30] Flammia, S. T. & Liu, Y.-K. Direct fidelity estimation from few Pauli measurements. *Phys. Rev. Lett.* **106**, 230501 (2011).
- [31] Ježek, M., Furášek, J. & Hradil, Z. c. v. Quantum inference of states and processes. *Phys. Rev. A* **68**, 012305 (2003).
- [32] Bylander, J. *et al.* Noise spectroscopy through dynamical decoupling with a superconducting flux qubit. *Nature Physics* **7**, 565–570 (2011).
- [33] Paik, H. *et al.* How coherent are Josephson junctions? Preprint at <http://arxiv.org/abs/1105.4652> (2011).